

N -resonances in a buffered micrometric Rb cell: splitting in a strong magnetic field

Armen Sargsyan¹, Rafayel Mirzoyan^{1,2}, Aram Papoyan^{1*}, and David Sarkisyan¹

¹*Institute for Physical Research, NAS of Armenia,
Ashtarak-2, 0203, Armenia*

²*Laboratoire Interdisciplinaire Carnot de Bourgogne, UMR CNRS 6303, Université' de Bourgogne,
21078 Dijon Cedex, France*

*Corresponding author: papoyan@ipr.sci.am

Compiled November 12, 2018

N -resonances excited in rubidium atoms confined in micrometric-thin cells with variable thickness from $1\ \mu\text{m}$ to $2\ \text{mm}$ are studied experimentally for the cases of a pure Rb atomic vapor and of a vapor with neon buffer gas. Good contrast and narrow linewidth were obtained for thicknesses as low as $30\ \mu\text{m}$. The higher amplitude and sharper profile of N -resonances in the case of a buffered cell was exploited to study the splitting of the ^{85}Rb D_1 N -resonance in a magnetic field of up to $2200\ \text{G}$. The results are fully consistent with the theory. The mechanism responsible for forming N -resonances is discussed. Possible applications are addressed. © 2018 Optical Society of America

OCIS codes: 020.1335, 300.6360.

The formation of narrow optical resonances via coherent processes continues to be of high interest because its fascinating properties have potentially significant applications in quantum information, metrology, magnetometry, and other fields [1]. Though narrow resonances are predominantly formed by electromagnetically induced transparency (EIT) and the related phenomenon of coherent population trapping (CPT) in a Λ -system, other schemes are exploited as well: EIT in a “ladder” system, electromagnetically induced absorption (EIA), etc. It was shown in [2] that a so-called N -resonance that forms in a Λ -system of the Rb $D_{1,2}$ lines and manifests itself by an increase of the absorption (as it is for the EIA-resonance), can be competitive with the aforementioned resonances. The main advantage of this process is that it makes it technically easier to form a high-contrast, sub-natural resonance. In [3] it was demonstrated that better contrast could be attained for a D_2 N -resonance, while the linewidth was narrower for D_1 N -resonance. The possibility of light-shift cancellation, which might be important for atomic clock applications, was shown in [4]. The profile asymmetry of N -resonances was studied in [5]. The parameters of N -resonances can be improved by using laser radiation from three sources [6]. For applications in spectroscopy, metrology etc., it is important to reduce the dimensions of the atomic vapor cell in which optical resonances are formed while maintaining good resonance parameters [7–10]. In this letter we report on N -resonances observed with wedged micrometric-thin cells (MTC) filled with Rb vapor together with $150\ \text{Torr}$ of neon gas in magnetic fields of up to $2.2\ \text{kG}$. The thicknesses L of the MTCs ranged from $1\ \mu\text{m}$ to $50\ \mu\text{m}$ and from $40\ \mu\text{m}$ to $2\ \text{mm}$. The design of the MTCs used was similar to that presented in [10]. The N -resonance was formed in a Λ -system by two lasers

beam, whose frequency could be tuned, and the coupling beam, whose frequency was fixed. The diagram presented in the inset of Fig. 2 shows the Λ -system for the ^{85}Rb atom, where $F_g = 2,3$ are the ground levels, and the combined upper level $5P_{1/2}$ consists of hyperfine levels $F_e = 2,3$. The probe laser frequency ν_P was resonant with the $5S_{1/2}, F_g = 3 \rightarrow 5P_{1/2}$ transition, and the coupling laser frequency was shifted by the value of the ground state hyperfine splitting (Δ_{HFS}): $\nu_C = \nu_P - \Delta_{HFS}$. The experimental arrangement is sketched in Fig. 1.

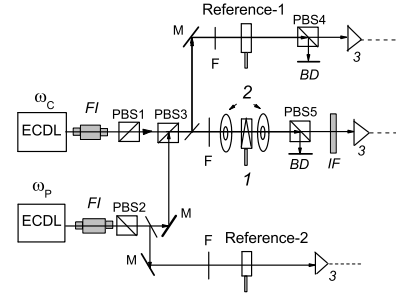


Fig. 1. Sketch of the experimental setup. ECDL- diode lasers; FI- Faraday isolator; 1- MTC in the oven; PBS- polarizing beam splitters; 2- permanent ring magnets; 3- photodetectors; IF- interference filter with $10\ \text{nm}$ transmission bandwidth at $795\ \text{nm}$; F- neutral density filters; BD- beam dump to block ν_c . PBS5 is used to single out ν_p for detection.

The beams of two single-frequency extended cavity diode lasers (ECDL) were carefully superimposed and directed by PBS3 onto the MTC. The coupling and probe beams were linearly polarized in orthogonal planes. The small thickness of MTC makes it possible to use a permanent ring magnet (PRM) in order to apply a strong magnetic field and still obtain a homogeneous field over

the thickness of the cell: in the MTC, the variation of the B -field inside the atomic vapor column is negligible compared to value of the applied magnetic field. The magnetic field was measured by a calibrated Hall gauge. To control the magnetic field value, one of the magnets was mounted on a micrometric translation stage that allowed longitudinal displacement. Portions of the coupling and probe beams were diverted to an auxiliary 40 μm -long Rb cell filled with Ne gas to obtain an N -resonance spectrum at $B = 0$. This spectrum served as frequency

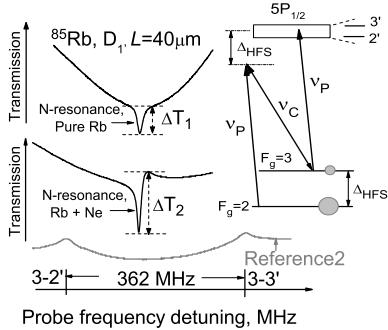


Fig. 2. Transmission spectra of the probe radiation through the MTC with $L = 40 \mu\text{m}$. Spectra containing an N -resonance are presented for two cases: pure Rb vapor (upper curve), which gave a linewidth of around 10 MHz, and Rb with 150 Torr Ne (lower curve), which gave a linewidth of around 8 MHz. Spectra were obtained under nearly identical conditions. For convenience, the spectra are shifted in the vertical direction. The lower grey curve is spectrum of Reference-2. Inset: relevant energy levels of ^{85}Rb involved in N -resonance formation.

Reference-1. Furthermore, another portion of the probe beam was diverted to a Rb nano-cell with $L = \lambda$ to obtain a $B = 0$ transmission spectrum, which served as frequency Reference 2 [11]. The optical radiation signals recorded by photodiodes (3) were amplified and recorded by a four-channel digital storage oscilloscope.

Although the best N -resonance contrast and linewidth can be achieved for cells with thicknesses around 1 cm [2–6], using an MTC with a thickness as small as 30 to 40 μm still allowed us to obtain good resonance parameters. The experimentally recorded N -resonance spectra are presented in Fig. 2. The MTC side arm, whose temperature determines the density of Rb atoms, was maintained at $\sim 110^\circ\text{C}$ (Rb atomic vapor density 10^{13}cm^{-3}). In the case of the pure Rb vapor (the upper curve) the change of the probe transmission over the N -resonance was $\Delta T_{\text{Rb}} \approx 7\%$, and its lineshape was symmetric. For the buffered cell (the lower curve) the change was larger ($\Delta T_{\text{Rb+Ne}} \approx 12\%$), and the N -resonance shape was asymmetric, consistent with the results reported in [5]. However, the sharp profile of the transmission signal in this case makes it convenient for studying the splitting of N -resonances in a magnetic field. The N -resonance was split into 5 components in a magnetic field. This splitting is shown in Fig. 3 for the B -field range from 59 G to

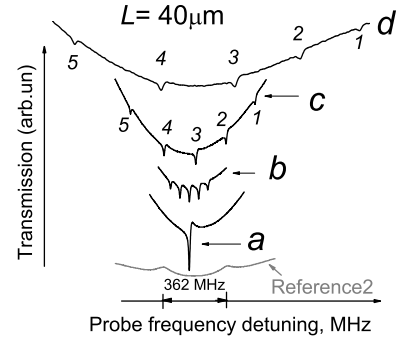


Fig. 3. Splitting of the N -resonance in a moderate B -field. a: spectrum of Reference-1 for $B = 0$; b - d: N -resonance spectra for $B = 59 \text{ G}$ (b), 190 G (c), and 460 G (d). The labels 1-5 denote corresponding transitions shown in Fig. 6. The lower grey curve shows spectrum of Reference-2.

460 G. The coupling and probe beam powers were 4 mW and 1 mW, with a beam diameter of 1.5 mm.

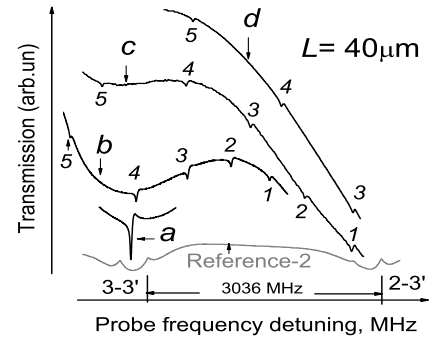


Fig. 4. Splitting of the N -resonance in a strong B -field. a: spectrum of Reference-1 for $B = 0$; b - d: N -resonance spectra for $B = 808 \text{ G}$ (b), 1238 G (c), and 1836 G (d). The labels 1-5 denote corresponding transitions shown in Fig. 6. The lower grey curve shows spectrum of Reference-2.

Spectra showing splitting for stronger B -field values (808 - 1836 G) are presented in Fig. 4. Although the amplitudes of the N -resonance components tended to decrease with B , they were nevertheless easily observable up to $B = 2200 \text{ G}$. As can be seen from Fig. 3 and Fig. 4, the narrow linewidth of the N -resonance makes it possible to achieve a spectral resolution that is higher by a factor of 5 as compared with the results obtained by the λ -Zeeman technique [9].

Figure 5 presents the dependence of the frequency of the magnetic sublevels of the ^{85}Rb $F_g=2,3$ ground hyperfine states on the magnetic field, as calculated by a well-known model (see, for example, [11]). The system is described in the basis of F, m_F in the low-field (Zeeman) regime, and in the basis of m_J, m_I in the strong-field (hyperfine Paschen-Back [HPB]) regime, when $B \gg 700 \text{ G}$ [9]. N -resonance components are observed whenever the 2-photon resonance conditions are

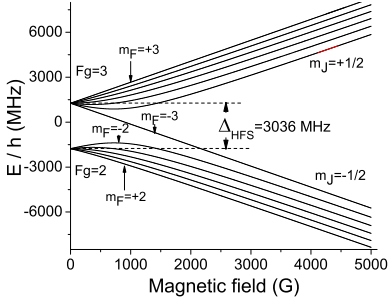


Fig. 5. Splitting of $^{85}\text{Rb } 5S_{1/2}$ ground level hyperfine structure in an external magnetic field.

satisfied: $\nu_P - \nu_C = [E(F=3, m_F) - E(F=2, m_F)]/h$.

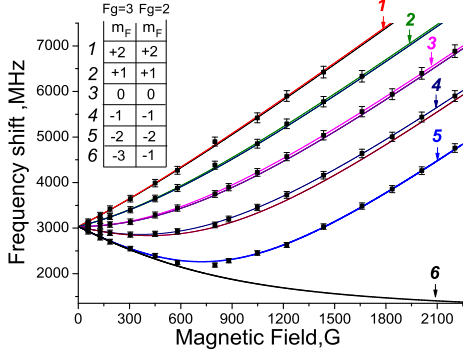


Fig. 6. Frequency shifts of the N -resonance components in a B -field. *Solid lines*: theory; *symbols*: experiment. The inaccuracy does not exceed 2%. The initial and final Zeeman sublevels of $F_g=2,3$ are indicated in the Table for components 1-5.

Figure 6 shows the magnetic field dependence of the frequency shift for the five observed N -resonance components. Other N -resonance components expected from the calculations and presented as thin solid lines in Fig. 6 are not observable in the experiment because at low fields ($B < 500$ G) their separation from components 1-5 is unresolvably small (several MHz), while at high fields the atomic transition probabilities (line strengths) are reduced (either for the coupling or for the probe radiation) down to undetectable values (see component 6, undetectable at $B > 500$ G). Note that the slope of components 1-5 contains contributions from the B -field shifts of the corresponding ground-state Zeeman sublevels $F_g=2,3$ (see Fig. 5). Thus, N -resonance component 1 has the largest slope of 2.68 MHz/G in the region around 2 kG, that is, $|-1.34|$ MHz/G from $F_g=2$, $m_F=+2$, and $|+1.34|$ MHz/G from $F_g=3$, $m_F=+2$. For $B > 1.5$ kG an HPB regime becomes predominant. As a consequence, the slopes of components 1-5 tend to equalize at the same final value of ~ 2.8 MHz/G.

The studies presented above indicate that $F_g=2$ is the initial, and $F_g=3$ is the final level for the N -resonance. Based on these results, we believe the following physical mechanism is responsible for the origin

of the N -resonance. The probe radiation causes strong optical pumping, which transfers a large number of Rb atoms from the $F_g=3$ state to the $F_g=2$ state. The presence of buffer gas enhances efficiency of optical pumping, yet weakly influences the spectral broadening (at the given pressure). In consequence, an $N_2 > N_3$ population condition is assured (where N_2 and N_3 are the populations of the $F_g=2$ and $F_g=3$ levels, respectively). This condition is schematically indicated by the large and small circles in the inset of Fig. 2. When the condition $\nu_P - \nu_C = \Delta_{HFS}$ is satisfied, a strong two-photon absorption of the probe radiation $F_g=2 \rightarrow F_g=3$ occurs at the frequency $\nu_P = \nu_C + \Delta_{HFS}$, which results in the formation of an N -resonance.

Note that the 30 μm -thick Rb cell could be used to map strongly inhomogeneous magnetic fields with high spatial resolution. In particular, for a B -field gradient of around 100 G/mm, the displacement of the MTC by 30 μm results in a frequency shift of the N -resonance component labeled 1 of around 8 MHz, which is easy to detect because of its sharp profile.

We thank F. Gahbauer for useful discussions.

References

1. M. Fleischhauer, A. Imamoglu, and J. P. Marangos, *Rev. Mod. Phys.* **77**, 633–673 (2005).
2. A. S. Zibrov, C. Y. Ye, Y. V. Rostovtsev, A. B. Matsko, and M. O. Scully, *Phys. Rev. A* **65**, 043817 (2002).
3. I. Novikova, D. F. Phillips, A. S. Zibrov, R. L. Walsworth, A. V. Taichenachev, and V. I. Yudin, *Opt. Lett.* **31**, 2353–2355 (2006).
4. I. Novikova, D. F. Phillips, A. S. Zibrov, R. L. Walsworth, A. V. Taichenachev, and V. I. Yudin, *Opt. Lett.* **31**, 622–624 (2006).
5. C. Hancox, M. Hohensee, M. Crescimanno, D. F. Phillips, and R. L. Walsworth, *Opt. Lett.* **33**, 1536–1538 (2008).
6. I. Ben-Aroya, G. Eisenstein, *Opt. Express* **19**, 9956 (2011).
7. S. Knappe, P. Schwindt, V. Shah, L. Hollberg, J. Kitching, L. Liew, J. Moreland, *Opt. Express* **13**, 1249 (2005).
8. T. Baluktian, C. Urban, T. Bublat, H. Giessen, R. Löw, T. Pfau, *Opt. Lett.* **35**, 1950–1952 (2010).
9. A. Sargsyan, G. Hakhumyan, C. Leroy, Y. Pashayan-Leroy, A. Papoyan, D. Sarkisyan, *Opt. Lett.* **37**, 1379 (2012).
10. G. Hakhumyan, A. Sargsyan, C. Leroy, Y. Pashayan-Leroy, A. Papoyan, D. Sarkisyan, *Opt. Express* **18**, 14577 (2010).
11. M. Auzinsh, D. Budker, S.M. Rochester, Oxford University Press: ISBN 978-0-19-956512-2 (2010).

References

1. M. Fleischhauer, A. Imamoglu, and J. P. Marangos, “Electromagnetically induced transparency: Optics in coherent media,” *Rev. Mod. Phys.* **77**, 633–673 (2005).
2. A. S. Zibrov, C. Y. Ye, Y. V. Rostovtsev, A. B. Matsko, and M. O. Scully, “Observation of a three-photon electromagnetically induced transparency in hot atomic vapor,” *Phys. Rev. A* **65**, 043817 (2002).
3. I. Novikova, D. F. Phillips, A. S. Zibrov, R. L. Walsworth, A. V. Taichenachev, and V. I. Yudin, “Comparison of 87Rb N-resonances for D1 and D2 transitions,” *Opt. Lett.* **31**, 2353–2355 (2006).
4. I. Novikova, D. F. Phillips, A. S. Zibrov, R. L. Walsworth, A. V. Taichenachev, and V. I. Yudin, “Cancellation of light shifts in an N-resonance clock,” *Opt. Lett.* **31**, 622–624 (2006).
5. C. Hancox, M. Hohensee, M. Crescimanno, D. F. Phillips, and R. L. Walsworth, “Lineshape asymmetry for joint coherent population trapping and three-photon N resonances,” *Opt. Lett.* **33**, 1536–1538 (2008).
6. I. Ben-Aroya, G. Eisenstein, “Observation of large contrast electromagnetically induced absorption resonance due to population transfer in a three-level Λ -system interacting with three separate electromagnetic fields,” *Optics Express* **19**, 9956 (2011).
7. S. Knappe, P. Schwindt, V. Shah, L. Hollberg, J. Kitching, L. Liew, J. Moreland, “A chip-scale atomic clock based on 87Rb with improved frequency stability,” *Opt. Express* **13**, 1249 (2005).
8. T. Baluktsian, C. Urban, T. Bublat, H. Giessen, R. Löw, T. Pfau, “Fabrication method for microscopic vapor cells for alkali atoms,” *Opt. Lett.* **35**, 1950–1952 (2010).
9. A. Sargsyan, G. Hakhumyan, C. Leroy, Y. Pashayan-Leroy, A. Papoyan, D. Sarkisyan, “Hyperfine Paschen-Back regime realized in Rb nanocell,” *Opt. Lett.* **37**, 1379 (2012).
10. G. Hakhumyan, A. Sargsyan, C. Leroy, Y. Pashayan-Leroy, A. Papoyan, D. Sarkisyan, “Essential Features of Optical Processes in Rb submicron Thin Cell Filled with Neon Gas,” *Opt. Express.* **18**, 14577 (2010).
11. M. Auzinsh, D. Budker, S.M. Rochester, “Optically Polarized Atoms: Understanding Light-Atom Interactions,” Oxford University Press: ISBN 978-0-19-956512-2 (2010).